JOURNAL OF AIRCRAFT
Vol. 33, No. 4, July–August 1996

State-Space Modeling for Aeroelastic Panels with Linearized Potential Flow Aerodynamic Loading

Kenneth D. Frampton,* Robert L. Clark,† and Earl H. Dowell‡
Duke University, Durham, North Carolina 27708

This article presents a new method for the state-space modeling of aeroelastic panels subject to linearized potential flow aerodynamic loading. This is accomplished by approximating the aerodynamic generalized forces on the panel with discrete, infinite impulse response (IIR) filters. The IIR filters are created using Prony's method for a least-squares-fit to the aerodynamic influence functions. These filters are coupled to the in vacuo panel dynamic system as feedback, creating a coupled, aeroelastic system. The accuracy of the model is established by comparing the panel flutter boundaries of the approximate system with those found in past studies.

Nomenclature

A, B, F, G = state-space matrices
a = panel length, chord
$a_i, \hat{a}_i$ = filter coefficients
a_∞ = speed of sound
b = panel width, span
$b_i, \hat{b}_i$ = filter coefficients
D = $EI/(1-\nu^2)$, panel stiffness
D_{mn} = aerodynamic influence coefficient
$H_{mn}(t)$ = aerodynamic influence function
h = panel thickness
I = approximate infinite impulse response filter order
$I_{mn}(t)$ = aerodynamic influence function
$J_1[\cdot]$ = Bessel's function
M = Mach number
M_n = modal mass
N = number of expansion modes
$P(z)$ = exact z transfer function
$\hat{P}(z)$ = approximate z transfer
$\hat{P}(\kappa)$ = approximate Laplace transfer function
$p(x, y, t)$ = aerodynamic pressure
$Q_n(t)$ = generalized force
$q_n(t)$ = generalized coordinate
R = finite impulse response filter order
$r_n(s)$ = $q_n(t)/h$
S_{mn} = aerodynamic influence coefficient
s = tU_∞/a
T = sample period
t = time
U_a = freestream velocity
$\boldsymbol{u}$ = state-space input vector
$w(x, y, t)$ = panel displacement
x, y, z = Cartesian coordinates
$\boldsymbol{x}$ = state vector
$\boldsymbol{y}$ = output vector
α, γ = Fourier transform variables
κ = Laplace domain variable
λ = $\rho U_a^2 a^3/D$
μ = $\rho_a a/\rho_p$
ρ_a = density of fluid
ρ_p = panel mass per area
τ = integration dummy variable
$\phi(x, y, z, t)$ = fluid velocity potential
$\Psi_n(x, y)$ = modal expansion functions
ω_n = modal natural frequency

Subscripts
a = aerodynamic
m, n = modal indices
p = panel

Received May 21, 1995; revision received Dec. 2, 1995; accepted for publication Dec. 29, 1995.

*Graduate Research Assistant, Department of Mechanical Engineering and Materials Science. Student Member AIAA.
†Assistant Professor, Department of Mechanical Engineering and Materials Science. Member AIAA.
‡J. A. Jones Professor and Dean, School of Engineering. Fellow AIAA.

Introduction

PANEL flutter is the self-excited dynamic instability of plate-like structures exposed to fluid flow. This aeroelastic phenomenon has received much attention in the past and is very important toward the successful development of supersonic aircraft such as the National Aerospace Plane, the High Speed Civil Transport, and the Advanced Tactical fighter, to name a few. Dugundji[1] published an excellent paper on early investigations into linear panel flutter, whereas Gray and Mei[2] gave a review of more recent efforts including nonlinear effects. However, the vast majority of work has been performed assuming piston theory as the aerodynamic model. The use of piston theory is not without good reason, since it is reasonably accurate at higher Mach numbers and modeling the effects of linearized potential flow, which is necessary for lower Mach numbers ($M < 1.5$), is challenging. Since low supersonic flight speeds are utilized by many aircraft, it is important to consider the effects of full potential flow aerodynamic loading in panel flutter investigations.

The few references that include linearized potential flow aerodynamics focus on the determination of flutter boundaries, and subsequently, the limit cycle oscillations in the postflutter (nonlinear) regime. These models, however, are not conducive to the application of modern control theory. A method of building a state-space model of the coupled aeroelastic system would permit the determination of flutter boundaries as well as provide a means of applying modern control theory to the problem. While this has already been accomplished for typical wing sections,[3,4] it has yet to be done for panels.

This article presents a method for constructing a state-space model of the coupled aeroelastic panel including linearized potential flow aerodynamics. This is accomplished by approximating the aerodynamic generalized forces on a panel, as developed by Dowell,[5,6] with discrete, infinite impulse response

(IIR) filters. These filters are coupled to the in vacuo panel dynamic system as feedback, creating a coupled, aeroelastic system. The accuracy of the model is established by comparing the panel flutter boundaries of the approximate system with those found in the literature.[6-9]

Panel Dynamics and Generalized Forces

The partial differential equation (PDE) of motion describing a thin, uniform panel is[10]

$$D\left[\frac{\partial^4 w(x, y, t)}{\partial x^4} + \frac{\partial^4 w(x, y, t)}{\partial x^2 \partial y^2} + \frac{\partial^4 w(x, y, t)}{\partial y^4}\right] + \rho_p \frac{\partial^2 w(x, y, t)}{\partial t^2} + p(x, y, t) = 0 \tag{1}$$

The coordinate system for the panel is shown in Fig. 1.

A separable expansion solution is assumed using the in vacuo orthogonal panel eigenfunctions and generalized coordinates:

$$w(x, y, t) = \sum_{n=1}^{N} \Psi_n(x, y) q_n(t) \tag{2}$$

Substituting Eq. (2) into Eq. (1), multiplying by an arbitrary expansion function $\Psi_m(x, y)$, and integrating over the domain yields a set of ordinary differential equations of the form:

$$M_n[\ddot{q}_n(t) + \omega_n^2 q_n(t)] + \rho_a U_a^2 Q_n(t) = 0 \tag{3}$$

where

$$M_n = \int_0^b \int_0^a \rho_p \Psi_n \Psi_m \, dx \, dy \tag{4}$$

$$M_n \omega_n^2 = \int_0^b \int_0^a D\left[\frac{\partial^2 \Psi_n}{\partial x^2}\frac{\partial^2 \Psi_m}{\partial x^2} + \nu\left(\frac{\partial^2 \Psi_n}{\partial x^2}\frac{\partial^2 \Psi_m}{\partial y^2} + \frac{\partial^2 \Psi_m}{\partial x^2}\frac{\partial^2 \Psi_n}{\partial y^2}\right) + 2(1-\nu^2)\frac{\partial^2 \Psi_n}{\partial x \partial y}\frac{\partial^2 \Psi_m}{\partial x \partial y} + \frac{\partial^2 \Psi_n}{\partial y^2}\frac{\partial^2 \Psi_m}{\partial y^2}\right] dx \, dy \tag{5}$$

and the generalized forces are a function of the aerodynamic pressure

$$Q_n(t) = \int_0^b \int_0^a \frac{p(x, y, t)}{\rho_a U_a^2} \Psi_n(x, y) \, dx \, dy \tag{6}$$

Full Potential Flow Generalized Forces

Consider the case of a simply supported panel with the following eigenfunctions (only one mode in the y direction for simplicity such that $n = 1, 2, \ldots, N$):

$$\Psi_n(x, y) = \sin[(n\pi/a)x]\sin[(\pi/b)y] \tag{7}$$

In this case, the panel equation of motion, Eq. (3), can be expressed nondimensionally as

$$\ddot{r}_n(s) + (\mu/\lambda)\pi^4[n^2 + (a/b)^2]^2 r_n(s) + 4\mu Q_n(s) = 0 \tag{8}$$

The generalized forces $Q_n(t)$ are found by solving the PDE describing the velocity potential in an inviscid, irrotational fluid moving parallel to the x axis

$$\nabla^2 \phi - \frac{1}{a_\infty^2}\left(\frac{\partial^2 \phi}{\partial t^2} + 2U_a \frac{\partial^2 \phi}{\partial x \partial t} + U_a^2 \frac{\partial^2 \phi}{\partial x^2}\right) = 0 \tag{9}$$

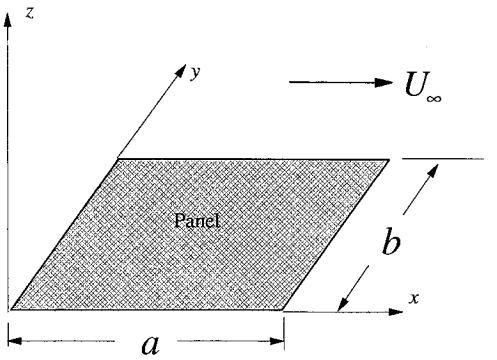

Fig. 1 Panel coordinate system.

subject to the boundary conditions for a panel embedded in an infinite baffle

$$\left.\frac{\partial \phi}{\partial z}\right|_{z=0} = \begin{cases} \dfrac{\partial w}{\partial t} + U_a \dfrac{\partial w}{\partial x} & \text{on the panel} \\ 0 & \text{off the panel} \end{cases} \tag{10}$$

and a finiteness or radiation condition as z approaches infinity.

The solution can be obtained by taking a Laplace transform with respect to time and a double Fourier transform with respect to the x and y spatial coordinates. The transformation is applied to Eqs. (9) and (10) and Bernoulli's equation,

$$p = -\rho_a\left(\frac{\partial \phi}{\partial t} + U_a \frac{\partial \phi}{\partial x}\right) \tag{11}$$

while incorporating Eq. (2). Details of the solution are discussed by Dowell.[5,6]

The solution yields the generalized aerodynamic forces on the panel, which are given here as

$$Q_n(t) = \sum_{m=1}^{N} Q_{mn}(t) \tag{12a}$$

where $Q_{mn}(t)$ is the force on the nth panel mode because of the motion of the mth panel mode, such that

$$Q_{mn}(t) = q_m(t)S_{mn} + \dot{q}_m(t)D_{mn} + \int_0^t q_m(\tau)H_{mn}(t-\tau)\, d\tau + \int_0^t \dot{q}_m(\tau)I_{mn}(t-\tau)\, d\tau \tag{12b}$$

$$S_{mn} = \frac{1}{M}\int_0^a \int_0^b \frac{\partial \Psi_m}{\partial x}\Psi_n \, dy \, dx \tag{12c}$$

$$D_{mn} = \frac{1}{MU_a}\int_0^a \int_0^b \Psi_m \Psi_n \, dy \, dx \tag{12d}$$

$$H_{mn}(t) = -\frac{U_a}{4\pi^2 M^2}\int_{-\infty}^{\infty}\int_{-\infty}^{\infty} G_{mn} i\alpha\sqrt{\alpha^2+\gamma^2}\, e^{-i\alpha U_a t} \times J_1(a_\infty t\sqrt{\alpha^2+\gamma^2})\, d\alpha \, d\gamma \tag{12e}$$

$$I_{mn}(t) = -\frac{1}{4\pi^2 M^2}\int_{-\infty}^{\infty}\int_{-\infty}^{\infty} G_{mn}\sqrt{\alpha^2+\gamma^2}\, e^{-i\alpha U_a t} \times J_1(a_\infty t\sqrt{\alpha^2+\gamma^2})\, d\alpha \, d\gamma \tag{12f}$$

$$G_{mn} = \int_0^a \int_0^b \Psi_m(x, y) e^{-i(\alpha x + \gamma y)}\, dy \, dx \times \int_0^a \int_0^b \Psi_n(x, y) e^{i(\alpha x + \gamma y)}\, dy \, dx \tag{12g}$$

The integrals in Eqs. (12c), (12d), and (12g) can be performed analytically for most panel eigenfunctions. Equations (12e) and (12f), which define the aerodynamic influence functions, must be evaluated numerically.

Piston Theory Generalized Forces

Piston theory is presented here for comparison with the full potential flow solution developed previously. Piston theory assumes that the pressure acting on the panel is equivalent to the pressure acting on a piston in a tube:

$$p = \rho_a a_\infty \left(\frac{\partial w}{\partial t} + U_a \frac{\partial w}{\partial x} \right) \tag{13}$$

The total piston velocity includes a convection term $U_a(\partial w/\partial x)$, as well as a direct velocity term $\partial w/\partial t$. Here the plate is the equivalent piston and the tube is perpendicular to the plate.

Combining Eqs. (2) and (13) and inserting into Eq. (6) yields the piston theory generalized aerodynamic forces

$$Q_n(t) = \sum_{m=1}^{N} Q_{mn}(t) \tag{14a}$$

where

$$Q_{mn}(t) = q_m(t) S_{mn} + \dot{q}_m(t) D_{mn} \tag{14b}$$

$$S_{mn} = \frac{1}{M} \int_0^a \int_0^b \frac{\partial \Psi_m}{\partial x} \Psi_n \, dy \, dx \tag{14c}$$

$$D_{mn} = \frac{1}{MU_a} \int_0^a \int_0^b \Psi_m \Psi_n \, dy \, dx \tag{14d}$$

Note that this result is identical to that obtained from full potential flow analysis if the influence functions [$H_{mn}(t)$ and $I_{mn}(t)$] are ignored.

Approximate Generalized Forces

Many techniques for approximating the aerodynamic loads on structures (mainly wing sections) have been published in the past. Jones[11] was one of the earliest, whereas Leishman[12] and Morino et al.[3] have more recently investigated Laplace/frequency domain approximations of the aerodynamic loads. However, the form of the aerodynamic forces expressed in Eqs. (12) does not lend itself to direct application of these methods. Utilization of the techniques in Refs. 1, 9, and 10 would require transforming the time domain representations in Eqs. (12) to the frequency domain. This additional computational step would introduce more error into the solution. Therefore, a more direct time domain approximation technique was sought.

Since the generalized aerodynamic forces represented in Eq. (12b) are functions of the panel generalized coordinates, they can be viewed as dynamic feedback on the panel. These feedback dynamics are characterized by the influence functions $H_{mn}(t)$ and $I_{mn}(t)$, which represent aerodynamic impulse responses, and the influence coefficients S_{mn} and D_{mn}, which are instantaneous or feedthrough dynamics.

Since there is no closed-form solution for the generalized forces, some approximation must be made. The approach suggested here is to construct digital filters that approximate these dynamics. A finite impulse response (FIR) filter of the form:

$$P(z) = \sum_{i=0}^{R-1} h(iT) z^{-i} \tag{15}$$

exactly represents a dynamic system having a discrete time impulse response $h(iT)$ and a z-domain transfer function $P(z)$ (Ref. 13). In this case the dynamic system is the aerodynamics represented by Eq. (12b), which has two impulse responses of $H_{mn}(iT)$ and $I_{mn}(iT)$. Note that $H_{mn}(iT)$ and $I_{mn}(iT)$ are discrete time approximations of Eqs. (12e) and (12f).

Equation (15) can be used to represent the aerodynamics of Eq. (12b) by substituting a numerically calculated influence function [$H_{mn}(iT)$ or $I_{mn}(iT)$] for $h(iT)$ in Eq. (15). However, constructing a state-space model of an FIR filter requires as many states as filter coefficients. Therefore, any reasonable discrete temporal resolution of the influence functions would result in a very high-order state-space model.

Fortunately, a reduced order recursive filter may be constructed by applying Prony's method to the influence functions.[14,15] Prony's method approximates an impulse response (in this case the influence functions) with a set of exponential functions in a least-squares sense. These exponential approximations to the influence functions can be readily transformed into an Ith order IIR filter of the form:

$$\hat{P}_{mn}(z) = \sum_{i=0}^{I-1} a_i z^{-i} \Big/ \sum_{i=0}^{I-1} b_i z^{-i} \tag{16}$$

Equating like powers of the FIR representation in Eq. (15) with the IIR representation of Eq. (16), and replacing the temporal argument iT with subscripts, yields an overdetermined set of equations (for $R >> I$) of the form:

$$\left\{ \frac{a}{0} \right\} = \left[\frac{h_1}{h_2} \right] \{b\} \tag{17a}$$

where

$$\left\{ \frac{a}{0} \right\} = \left\{ \begin{array}{c} a_0 \\ a_1 \\ \vdots \\ a_{I-1} \\ \hline 0 \\ 0 \\ \vdots \\ 0 \end{array} \right\} \tag{17b}$$

$$\left[\frac{h_1}{h_2} \right] = \left[\begin{array}{cccc} h_0 & 0 & \cdots & 0 \\ h_1 & h_0 & \cdots & 0 \\ \vdots & \vdots & & \vdots \\ h_{I-1} & h_{I-2} & \cdots & 0 \\ \hline h_I & h_{I-1} & \cdots & h_0 \\ h_{I+1} & h_I & \cdots & h_1 \\ \vdots & & \vdots & \vdots \\ h_{R-1} & h_{R-2} & \cdots & h_{R-I-1} \end{array} \right] \tag{17c}$$

$$\{b\} = \left\{ \begin{array}{c} b_0 \\ b_1 \\ \vdots \\ b_{I-1} \end{array} \right\} \tag{17d}$$

The lower portion of this system of equations, $0 = h_2 b$ is solved, in a least-square sense, to give the denominator coefficients b_i in Eq. (16). Then the numerator coefficients a_i can be found uniquely from the upper portion of Eq. (17a), $a = h_1 b$.

At this point, the approximate filter of Eq. (16) can be converted to a continuous time (Laplace domain) representation through a bilinear transformation. This transformation is accomplished by substituting for z in Eq. (16) as follows:

$$z = \frac{1 + (T/2)\kappa}{1 - (T/2)\kappa} \tag{18}$$

Note that care should be taken in the selection of T. Significant errors can result if the sample period is not sufficiently small. Application of the bilinear transformation results in a continuous time filter of the form:

$$\hat{P}_{mn}(\kappa) = \sum_{i=0}^{I-1} \hat{a}_i \kappa^i \Big/ \sum_{i=0}^{I-1} \hat{b}_i \kappa^i \tag{19}$$

where $\hat{a}_i$ and $\hat{b}_i$ are new coefficients.

As an example, suppose the values of the influence function $H_{mn}(iT)$ are used to solve for the filter coefficients in Eq. (17a). When provided with an input signal that represents the panel generalized coordinate $q_m(iT)$, this filter would output an approximate convolution of $q_m(iT)$ with $H_{mn}(iT)$. Similarly, a filter could be constructed from $I_{mn}(iT)$ and provided with a signal representing $\dot{q}_m(iT)$. Summing the outputs of the two filters would yield an approximation to the dynamic portion of Eq. (12b). This process will be covered in more detail later.

The accuracy of this type of approximation is demonstrated in Fig. 2. This plot shows the generalized force Q_{11} for a unit step change in the generalized coordinate q_1, as represented in Eq. (12b). The results are presented for a panel of aspect ratio $a/b = 1.0$, mass ratio $\mu = 0.1$, and $M = 2.0$. Three curves are shown, one representing direct calculation from the influence function $H_{11}(iT)$, while the others represent the step response of an 8th- and 16th-order approximating filter with a sample period of $T = 0.1$. As one would expect, the higher-order filter yields higher accuracy. Other influence functions exhibit similar accuracy.

An approximate filter can be found, as shown previously, for each $H_{mn}(t)$ and $I_{mn}(t)$. A complete set of these filters can then be summed according to Eqs. (12a) and (12b). This would yield a dynamic system that has the generalized coordinates $q_m(t)$ and $\dot{q}_m(t)$ as the inputs, and the generalized aerodynamic forces $Q_n(t)$ as the outputs. This system is then coupled as

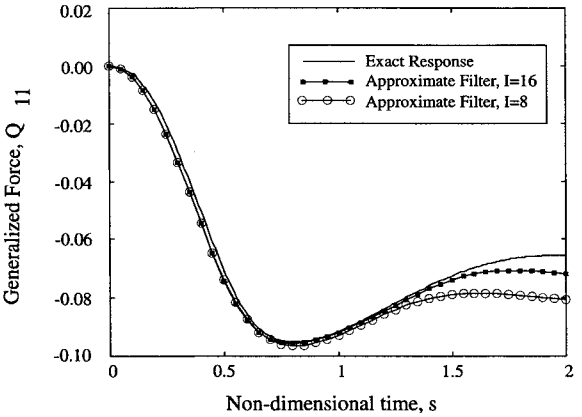

Fig. 2 Generalized force step response for exact and two approximating filters.

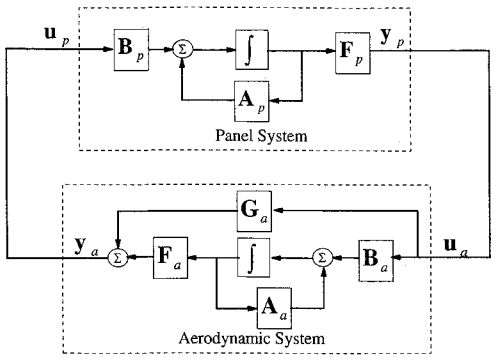

Fig. 3 State-space schematic of the complete aeroelastic system.

feedback on the panel resulting in a complete aeroelastic system. This is shown schematically (in state-space notation) in Fig. 3 and will be discussed in more detail in the next section.

State-Space Formulation

The general equation of motion for the panel, described in Eq. (3), in the absence of structural damping, can be expressed in state-space form as

$$\dot{\boldsymbol{x}}_p = A_p \boldsymbol{x}_p + B_p \boldsymbol{u}_p \tag{20a}$$

$$\boldsymbol{y}_p = F_p \boldsymbol{x}_p \tag{20b}$$

where

$$\boldsymbol{x}_p = \{q_1 \quad q_2 \quad \cdots \quad q_n \quad \dot{q}_1 \quad \dot{q}_2 \quad \cdots \quad \dot{q}_n\}^T \tag{20c}$$

$$A_p = \begin{bmatrix} 0 & 0 & \cdots & 0 & 1 & \cdots & 0 \\ \vdots & \vdots & \ddots & \vdots & \vdots & \ddots & \vdots \\ 0 & 0 & \cdots & 0 & 0 & \cdots & 1 \\ -\omega_1^2 & 0 & \cdots & 0 & 0 & \cdots & 0 \\ 0 & -\omega_2^2 & \cdots & 0 & 0 & \cdots & 0 \\ \vdots & \vdots & \ddots & \vdots & \vdots & \ddots & \vdots \\ 0 & 0 & \cdots & -\omega_n^2 & 0 & \cdots & 0 \end{bmatrix} \tag{20d}$$

$$B_p = \rho_a U_a^2 \begin{bmatrix} 0 & 0 & \cdots & 0 \\ 0 & 0 & \cdots & 0 \\ \vdots & & \ddots & \vdots \\ 0 & 0 & \cdots & 0 \\ \dfrac{-1}{M_1} & 0 & \cdots & 0 \\ 0 & \dfrac{-1}{M_2} & \cdots & 0 \\ \vdots & & \ddots & \vdots \\ 0 & 0 & \cdots & \dfrac{-1}{M_n} \end{bmatrix} \tag{20e}$$

$$\boldsymbol{u}_p = \{Q_1(t) \quad Q_2(t) \quad \cdots \quad Q_n(t)\}^T \tag{20f}$$

$$F_p = \begin{bmatrix} 1 & 0 & \cdots & 0 & 0 & 0 & \cdots & 0 \\ 0 & 0 & \cdots & 0 & 1 & 0 & \cdots & 0 \\ 0 & 1 & \cdots & 0 & 0 & 0 & \cdots & 0 \\ 0 & 0 & \cdots & 0 & 0 & 1 & \cdots & 0 \\ \vdots & \vdots & & \vdots & \vdots & \vdots & & \vdots \\ 0 & 0 & \cdots & 1 & 0 & 0 & \cdots & 0 \\ 0 & 0 & \cdots & 0 & 0 & 0 & \cdots & 1 \end{bmatrix} \tag{20g}$$

such that the output vector, which is equivalent to the input of the aerodynamic system, is a reordered version of the panel state vector:

$$\boldsymbol{y}_p = \{q_1 \quad \dot{q}_1 \quad q_2 \quad \dot{q}_2 \quad \cdots \quad q_n \quad \dot{q}_n\}^T \tag{20h}$$

A filter of the form in Eq. (19) can be cast in state variable form as follows:

$$\boldsymbol{x}_{\hat{P}} = A_{\hat{P}} \boldsymbol{x}_{\hat{P}} + B_{\hat{P}} \boldsymbol{u}_{\hat{P}} \tag{21a}$$

$$\boldsymbol{y}_{\hat{P}} = F_{\hat{P}} \boldsymbol{x}_{\hat{P}} + G_{\hat{P}} \boldsymbol{u}_{\hat{P}} \tag{21b}$$

where

$$A_{\hat{P}} = \begin{bmatrix} -\hat{b}_2/\hat{b}_1 & -\hat{b}_3/\hat{b}_1 & \cdots & -\hat{b}_{I-1}/\hat{b}_1 & -\hat{b}_I/\hat{b}_1 \\ 1 & 0 & \cdots & 0 & 0 \\ 0 & 1 & \cdots & 0 & 0 \\ \vdots & \vdots & \ddots & \vdots & \vdots \\ 0 & 0 & \cdots & 1 & 0 \end{bmatrix} \tag{21c}$$

$$B_{\hat{P}} = \begin{bmatrix} 1 \\ 0 \\ \vdots \\ 0 \end{bmatrix} \tag{21d}$$

$$F_{\hat{P}} = [\hat{a}_2/\hat{b}_1 - \hat{a}_1\hat{b}_2/\hat{b}_1^2 \quad \hat{a}_3/\hat{b}_1 - \hat{a}_1\hat{b}_3/\hat{b}_1^2 \quad \cdots \quad \hat{a}_l/\hat{b}_1 - \hat{a}_1\hat{b}_l/\hat{b}_1^2] \tag{21e}$$

$$G_{\hat{P}} = [\hat{a}_1/\hat{b}_1] \tag{21f}$$

The input is the appropriate panel generalized coordinate and the output is the approximate convolution of the generalized coordinate and the influence function used in the filter calculation of Eq. (17a). The states of the previous system are of mathematical construct and have no physical significance.

At this point a representation of Eq. (12b) can be constructed for a single plate mode ($m = n$) as follows:

1) The appropriate influence functions $H_{mm}(iT)$ and $I_{mm}(iT)$ are found by the numeric integration of Eqs. (12e) and (12f).

2) Two filters are constructed by solving Eq. (17a) for the filter coefficients, one based on $H_{mm}(iT)$ and the other based on $I_{mm}(iT)$.

3) Each of these two filters is transformed to continuous time using Eq. (18) and cast in state variable form according to Eq. (21a). In general, the state variable representations associated with $H_{mn}(iT)$ and $I_{mn}(iT)$ will be referred to as the sets $\{A_{H_{mn}}, B_{H_{mn}}, F_{H_{mn}}, G_{H_{mn}}\}$ and $\{A_{I_{mn}}, B_{I_{mn}}, F_{I_{mn}}, G_{I_{mn}}\}$, respectively.

4) Finally, the state variable representations are combined according to Eq. (12b) as follows:

$$\dot{x}_a = A_a x_a + B_a u_a \tag{22a}$$

$$y_a = F_a x_a + G_a u_a \tag{22b}$$

where

$$y_a = Q_{mn}(t) \tag{22c}$$

$$u_a = \{q_m \quad \dot{q}_m\}^T \tag{22d}$$

$$A_a = \begin{bmatrix} A_{H_{mm}} & 0 \\ 0 & A_{I_{mm}} \end{bmatrix} \tag{22e}$$

$$B_a = \begin{bmatrix} B_{H_{mm}} & 0 \\ 0 & B_{I_{mm}} \end{bmatrix} \tag{22f}$$

$$F_a = [F_{H_{mm}} \quad F_{I_{mm}}] \tag{22g}$$

and the influence coefficients of Eqs. (12c) and (12d) are incorporated as follows:

$$G_a = [G_{H_{mm}} + S_{mm} \quad G_{I_{mm}} + D_{mm}] \tag{22h}$$

The previous representation would be sufficient if the panel model had only one mode. This would result in only one term in the sum given by Eq. (12a). Multiple panel modes require the extension of the previous representation to include all appropriate influence functions. This more general representation is as follows:

$$\dot{x}_a = A_a x_a + B_a u_a \tag{23a}$$

$$y_a = F_a x_a + G_a u_a \tag{23b}$$

where

$$y_a = \{Q_1(t) \quad Q_2(t) \quad \cdots \quad Q_n(t)\}^T \tag{23c}$$

$$u_a = \{q_1 \quad \dot{q}_1 \quad q_2 \quad \dot{q}_2 \quad \cdots \quad q_n \quad \dot{q}_n\}^T \tag{23d}$$

$$A_a = \begin{bmatrix} A_{H_{11}} & 0 & \cdots & 0 & 0 \\ 0 & A_{I_{11}} & \cdots & 0 & 0 \\ \vdots & \vdots & \ddots & \vdots & \vdots \\ 0 & 0 & \cdots & A_{H_{mn}} & 0 \\ 0 & 0 & \cdots & 0 & A_{I_{mn}} \end{bmatrix} \tag{23e}$$

$$B_a = \begin{bmatrix} B_{H_{11}} & 0 & \cdots & 0 & 0 \\ 0 & B_{I_{11}} & \cdots & 0 & 0 \\ \vdots & \vdots & \ddots & \vdots & \vdots \\ 0 & 0 & \cdots & B_{H_{1n}} & 0 \\ 0 & 0 & \cdots & 0 & B_{I_{1n}} \\ \vdots & \vdots & \vdots & \vdots & \vdots \\ B_{H_{m1}} & 0 & \cdots & 0 & 0 \\ 0 & B_{I_{m1}} & \cdots & 0 & 0 \\ \vdots & \vdots & \ddots & \vdots & \vdots \\ 0 & 0 & \cdots & B_{H_{mn}} & 0 \\ 0 & 0 & \cdots & 0 & B_{I_{mn}} \end{bmatrix} \tag{23f}$$

$$F_a = \begin{bmatrix} F_{H_{11}} & F_{I_{11}} & \cdots & F_{H_{1n}} & F_{I_{1n}} \\ F_{H_{21}} & F_{I_{21}} & \cdots & F_{H_{2n}} & F_{I_{2n}} \\ \vdots & \vdots & \ddots & \vdots & \vdots \\ F_{H_{m1}} & F_{I_{m1}} & \cdots & F_{H_{mn}} & F_{I_{mn}} \end{bmatrix} \tag{23g}$$

$$G_a = \begin{bmatrix} G'_{H_{11}} & G'_{I_{11}} & \cdots & G'_{H_{1n}} & G'_{I_{1n}} \\ G'_{H_{21}} & G'_{I_{21}} & \cdots & G'_{H_{2n}} & G'_{I_{2n}} \\ \vdots & \vdots & \ddots & \vdots & \vdots \\ G'_{H_{m1}} & G'_{I_{m1}} & \cdots & G'_{H_{mn}} & G'_{I_{mn}} \end{bmatrix} \tag{23h}$$

and the influence coefficients are incorporated as follows:

$$G'_{H_{mn}} = G_{H_{mn}} + S_{mn} \tag{23i}$$

$$G'_{I_{mn}} = G_{H_{mn}} + D_{mn} \tag{23j}$$

The panel and aerodynamic state-space models can then be coupled together as shown in Fig. 3.

The size of the state-space model can be further reduced by taking advantage of certain symmetries in the influence functions. The greatest reduction can be had by noting that $H_{mn} = -H_{nm}$ and $I_{mn} = -I_{nm}$. Furthermore, if more than one expansion mode is used in the spanwise direction for a simply supported plate, the influence functions can be indexed such that $H_{mn} \rightarrow H_{pqrs}$ and $I_{mn} \rightarrow I_{pqrs}$. In this case, those influence functions where $|q - s|$ is odd, are zero.

Results

To validate the coupled model, the system parameters were varied and the flutter boundaries were compared to results from the literature. Flutter boundaries were found by increasing the nondimensional dynamic pressure λ and calculating the coupled system eigenvalues. Flutter instability occurs when at least one of the system eigenvalues lies in the right half-plane.

This is demonstrated in Fig. 4, which shows the distribution of the system eigenvalues. Note the distribution of the approximate aerodynamic eigenvalues. Those eigenvalues associated with the panel modes are contained in the zoom region indicated in Fig. 4. These results are for a panel with $a/b = 1.0$, $\mu = 0.1$, $M = 2.0$, and using a four-mode expansion [i.e., $N = 4$ in Eq. (2)]. In this case, the frequency is nondimensionalized such that $k = (\omega a/U_a)(\lambda/\mu)^{1/2}$.

Figure 5 is an expanded view of the zoom region of Fig. 4 and depicts the pole migration with increasing dynamic pressure. In Fig. 5 eigenvalues at different dynamic pressure are connected with a line. Note the path of the complex conjugate eigenvalue pair as they enter the right half-plane. Also note that the only eigenvalues that experience significant migration are the complex conjugate pairs that are associated with the panel modes. One of these two migrating pairs is the eigenvalue that becomes unstable.

Another important piece of information that can be obtained from the eigenvalue locus in Fig. 5 is the frequency of flutter. In Fig. 5 the frequency of flutter is between the first and second natural frequencies of the panel. This is consistent with the results in Ref. 6.

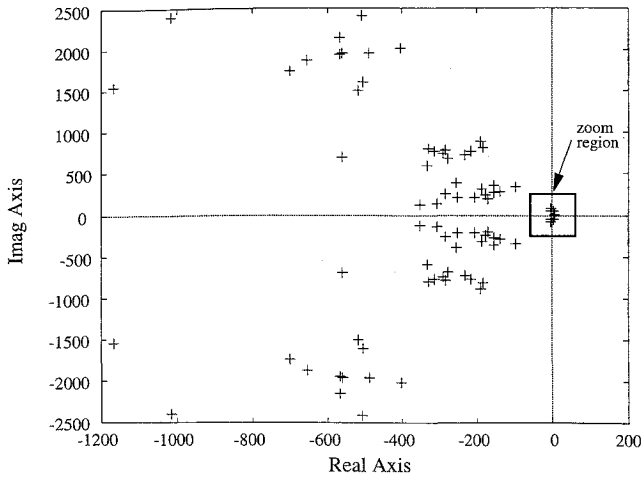

Fig. 4 Locus of system eigenvalues with varying dynamic pressure.

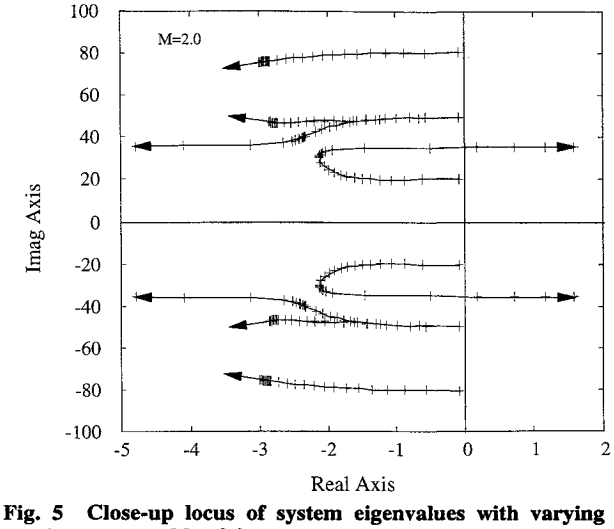

Fig. 5 Close-up locus of system eigenvalues with varying dynamic pressure, $M = 2.0$.

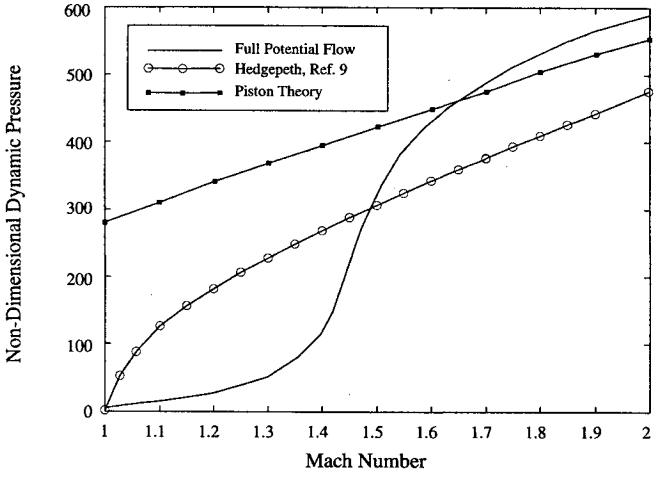

Fig. 6 Flutter dynamic pressure vs Mach number for $a/b = 0$.

A comparison of flutter dynamic pressure vs Mach number is shown in Fig. 6. Results are illustrated for a panel with $\mu = 0.1$ and $a/b = 0$ (i.e., an infinitely wide panel). Also included in the figure are the flutter boundaries for a piston theory model and for an approximate, quasisteady aerodynamic flutter boundary described by Hedgepeth.[9]

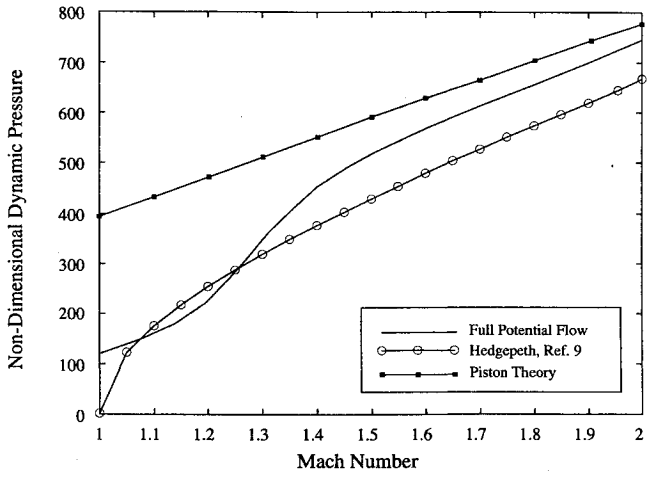

Fig. 7 Flutter dynamic pressure vs Mach number for $a/b = 1$.

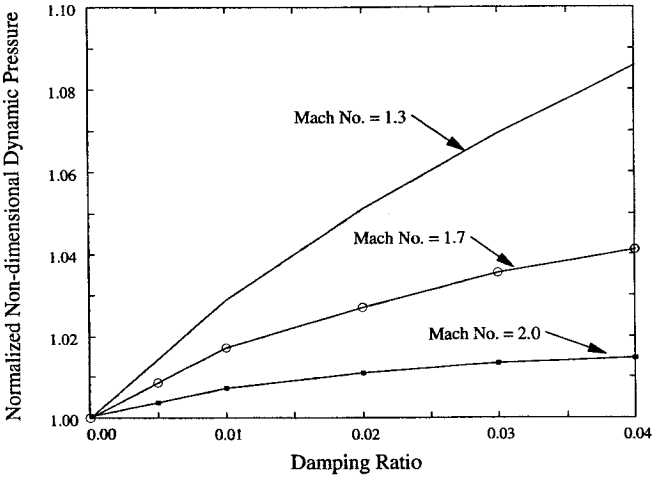

Fig. 8 Flutter dynamic pressure vs damping ratio.

Note in Fig. 6 that the three theories approach each other asymptotically as the Mach number increases. However, for Mach numbers below 1.5, the theory incorporating linearized potential flow aerodynamics predicts flutter boundaries well below the others. Full potential flow theory predicts a minimum flutter dynamic pressure of zero at a Mach number of 1.0. These results are consistent with those obtained by Dowell.[6,7]

A similar flutter boundary, for a square panel (i.e., $a/b = 1.0$) with $\mu = 0.1$ and using a four-mode expansion, is shown in Fig. 7. These results are also consistent with those obtained by Dowell. Note in this case the minimum flutter dynamic pressure is nonzero.

A final and interesting result is the effect of proportional modal damping on the flutter dynamic pressure. Figure 8 shows the flutter dynamic pressure, normalized with respect to the undamped flutter dynamic pressure, as a function of the modal damping ratio for three different Mach numbers. Proportional damping is modeled as an additional term of the form $2\zeta\omega_n\dot{q}_n$ to Eq. (3). Note that proportional damping has the greatest effect on flutter dynamic pressure at lower Mach numbers.

Conclusions

A new method for modeling the aerodynamic loading of panels that incorporates linearized potential flow aerodynamics has been developed. This was accomplished by approximating the aerodynamic generalized forces on the panel with discrete time filters. These filters were coupled as feedback to the in vacuo panel model. The accuracy of the method was demon-

strated by comparing results of this model with results obtained in previous work. Future work will use this new aeroelastic model in optimal control studies.

Acknowledgments

This work was supported in part by the Air Force Office of Scientific Research, Contract Monitor Jim Chang C.I.P.I., and the National Science Foundation Graduate Traineeship EE-92-56573.

References

[1]Dugundji, J., "Theoretical Considerations of Panel Flutter at High Supersonic Mach Numbers," *AIAA Journal*, Vol. 4, No. 7, 1966, pp. 1257–1266.

[2]Gray, C. E., and Mei, C., "Large Amplitude Finite Element Analysis of Composite Panels in Hypersonic Flow," *Proceedings of the AIAA Dynamics Specialist Conference*, AIAA, Washington, DC, 1992, pp. 127–132.

[3]Morino, L., Mastroddi, F., De Troia, R., Ghiringhelli, G. L., and Mantegazza, P., "Matrix Fraction Approach for Finite-State Aerodynamic Modeling," *AIAA Journal*, Vol. 33, No. 4, 1995, pp. 703–711.

[4]Leishman, J. G., and Nguyen, K. Q., "State-Space Representation of Unsteady Airfoil Behavior," *AIAA Journal*, Vol. 28, No. 5, 1989, pp. 836–844.

[5]Dowell, E. H., "Generalized Aerodynamic Forces on a Flexible Plate Undergoing Transient Motion," *Quarterly of Applied Mathematics*, Vol. 26, No. 3, 1967, pp. 2267–2270.

[6]Dowell, E. H., *Aeroelasticity of Plates and Shells*, Noordhoff International, Leyden, The Netherlands, 1975.

[7]Dowell, E. H., "Panel Flutter: A Review of the Aeroelastic Stability of Plates and Shells," *AIAA Journal*, Vol. 8, No. 3, 1970, pp. 385–399.

[8]Johns, D. J., "A Panel Flutter Review," *Manual on Aeroelasticity, Part III*, AGARD, 1969, Chap. 7.

[9]Hedgepeth, J. M., "Flutter of Rectangular Simply Supported Panels at High Supersonic Speeds," *Journal of the Aeronautical Sciences*, Vol. 24, No. 8, 1957, pp. 563–573.

[10]Meirovitch, L., *Analytical Methods in Vibrations*, Macmillan, New York, 1967.

[11]Jones, R. T., "The Unsteady Lift of a Wing of Finite Aspect Ratio," NACA Rept. 681, 1940.

[12]Leishman, J. G., "Validation of Approximate Indicial Aerodynamic Functions for Two-Dimensional Subsonic Flow," *Journal of Aircraft*, Vol. 25, No. 10, 1988, pp. 914–922.

[13]Haykin, S., *Adaptive Filter Theory*, 2nd ed., Prentice–Hall, Englewood Cliffs, NJ, 1991.

[14]Evans, A. G., and Fischl, R., "Optimal Least Squares Time-Domain Synthesis of Recursive Digital Filters," *IEEE Transactions on Audio and Electroacoustics*, Vol. AU-21, No. 1, 1973, pp. 61–65.

[15]Marple, S. L., *Digital Spectral Analysis with Applications*, Prentice–Hall, Englewood Cliffs, NJ, 1987.